Electronic Supplementary Material (ESI) for Analyst

Measuring and modelling cell-to-cell variation in uptake of gold nanoparticles

J. Charles. G. Jeynes, Christopher Jeynes, Michael J. Merchant, and Karen J. Kirkby*

Ion Beam Centre, University of Surrey, Guildford, Surrey, GU2 7XH

E-mail: j.c.jeynes@surrey.ac.uk

Phone: +44(0)1483 682242. Fax: +123 (0)123 4445557

Supporting Information Available

Glossary

Table S1: Glossary. *Note: "XRF" usually refers to fluorescence of X-rays with a primary X-ray beam, but the XRF mechanism can be excited by X-rays (XRF), electrons (SEM-EDS) or protons (PIXE). In all cases the X-rays excited (fluoresced) by the primary radiation will also excite secondary fluorescence by the XRF mechanism.

EBS:	elastic (non-Rutherford) backscattering spectrometry
EDS:	energy-dispersive X-ray spectrometry (used for PIXE, SEM and XRF analysis)
FBS:	foetal bovine serum
GNP:	gold nanoparticle
GUPIX:	PIXE spectrum analysis code from the University of Guelph
IBA:	Ion Beam Analysis (includes RBS, EBS, PIXE)
OMDAQ:	Oxford Microbeams digital data acquisition system for scanning ion microprobes
PBS:	phosphate-buffered saline
PIXE:	particle-induced X-ray emission
RBS:	Rutherford backscattering spectrometry
RPMI:	Roswell Park Memorial Institute
SEM:	scanning electron microscope/microscopy
TAT:	transactivator of transcription
TEM:	transmission electron microscope/microscopy
XRF:	X-ray fluorescence* (see note in caption)

Materials and Methods

GNPs-FBS non-specific binding and GNP-TAT conjugation

The GNPs were used as bought (British Biocell International, UK) with 30nm and 50nm diameter. These are citrate stabilised colloids.

The TAT peptide is a ten amino acid residue C(Nphys)ygrkkrrqrrr-NH2 (Anaspec Inc, USA), with an extra cysteine attached through a Nphys linker, providing the thiol linker moiety for covalent attachment to the gold nanoparticle. To avoid preciperation when the positively charged TAT peptide is added to the negatively charged GNPs, an oligonucleotide is first mixed with the TAT peptide. This is a randomly selected series of 17 bases; 5'-ATTGCTTGGCTTAACCA-3'. The oligo is mixed with the TAT peptide at a 2:1 volume ratio with both molecules at 1mg/ml. The

TAT:oligo is then mixed with GNPs at a ratio of 2:100. The GNPs are used at the manufacturers supplied concentration of 55 μg/ml gold. The TAT-GNP mixtures are thoroughly vortexed and left overnight for the thiol conjugation to take place before being used. GNP-TAT conjugates were mixed at a volume ratio of 1:10 with RPMI 1640 media (with 15% FBS) for cell culture, giving a final concentration of GNPs at 5.5 μg/ml.

For the FBS non-specific binding, the GNPs were mixed with 15 % FBS in RPMI at a volume ratio of 1:10, and left overnight. This mixture was diluted with 2:100 with deionised water (so that the concentration of GNPs is that same as the TAT samples), and then incubated with the the cells. The FBS contains a mixture of proteins essentially for cell growth, and these proteins non-specifically attach themselves to the GNPs, as shown by Chithrani *et al.* If the GNPs are first conjugated to TAT peptide, the FBS is effectively screened and non-specific binding is minimalised.

The cells were seeded at $1x10^5$ per 35 cm ^{2} in tissue culture treated petri dishs, and left with the GNPs-FBS or GNPs-TAT for 48 hours. The cells were then washed twice with phosphate buffered saline (PBS) to remove unbound GNPs and then prepared for microprobe analysis. This involved trypsinising the cells, pelleting them by 100g centrifugation and then fixing them in 4% paraformaldehyde. They were once again pelleted and then resuspended in double deionised water. The cells were finally pipetted onto a polypropylene stub and left to air dry in a fume hood before anaylsis.

Tissue culture

For tissue culture, RT112 bladder cancer cells (a gift from John Peacock, Kingston University, U.K.), were grown in RPMI 1640 media (Lonza, Wokingham, UK) with 15% fetal bovine serum (FBS), 2mM glutamine and 100 IU/ml penicillin & 1 μg/ml streptomycin incubated at 37 ^{o}C with 5% CO_2.

Ion Beam Analysis

In Figure S1 typical IBA spectra are shown. These are extracted offline from the list-mode files obtained from scanning microprobe analysis using the OMDAQ system. OMDAQ is designed primarily to handle PIXE spectra, and the X-ray spectrum fitting is effected using the state-of-the-art GUPIX code.[1] PIXE spectra (like all XRF spectra) need information about sample thickness to evaluate them accurately (because the X-ray line intensity is strongly affected by the self-absorption of the sample being analysed), but this depth profile information is explicitly present in the backscattered particle spectrum which is always available in parallel with PIXE data. OMDAQ was the first code to implement "Total IBA",[2] that is, the self-consistent treatment of PIXE and backscattering data;[3,4] nevertheless, the treatment of the particle spectra is quite rudimentary in OMDAQ, and excellent fits cannot usually be obtained. DataFurnace[5] is a code originally designed to handle particle spectra at state-of-the-art accuracy, and now also capable of a self-consistent treatment of PIXE spectra. In this case there is actually more information in the EBS spectra, and in this work we do not interpret the PIXE data closely.

We should mention here that the sample is imaged using the P K-line in the PIXE spectrum (see Fig.1), and the EBS signal does not have mass resolution to separate the P and S signals. Why not use the S K-line in the PIXE signal to disambiguate the EBS spectrum? Unfortunately the Au M-line (2.1-2.4 keV) overlaps the S K-line (2.31-2.46 keV) almost exactly and S cannot be analysed with any precision in the presence of Au. In this work we do not need to distinguish S and P very precisely since they are both matrix elements, and the EBS data is good enough to weigh the cells sufficiently accurately. Were this important we could analyse the PIXE and EBS spectrum self-consistently to determine from the PIXE spectrum how much P was in the combined S+P signal in the EBS spectrum. This is an iterative process because the relative proportion of S & P strongly affects the mutual absorption of the PIXE sigmals.

PIXE spectra are used to make the maps seen in Figure 1 to identify the cells. We collect data for about 10 hours for each region scan, allowing enough counts to clearly distinguish individual cells. The signal at the start and end of each run is identical indicating that no damage had been

done to the sample by the beam. The EBS spectrum from each cell is isolated and analysed individually. An example of an EBS spectrum from a single cell fitted with DataFurnace is shown in Figure S2a, and the fitted depth profile is shown in Figure S2b. Fitting assumed essentially a 2-layer sample of: cells on polypropylene foil; but what is not shown in the Figure S2b is any indication of the layer thickness inhomogeneity necessary to get good fits. To fit this inhomogeneity we use an equivalent "roughness" calculation.[6]

Note that the mass closure of the fits is almost 100% from the particle spectra, with only hydrogen being invisible. The H-content of the foil was assumed, and that of the cells was ignored - in any case the energy loss of the hydrogen in the cells will be relatively insignificant. Mass closure for XRF techniques usually suffers from instrumental factors: in this case the X-ray spectrum is cut off for energies lower than Si K by the thick filter used to exclude backscattered protons from the detector. Note also that depth is expressed in proper thin film units of mass per unit area. This is because the yield calibration for the particle spectrum is in terms of counts per unit energy loss in the spectrum, where the energy loss values are obtained from a linear combination of elemental energy losses (Bragg's rule[7]) which are tabulated in extensive semi-empirical tables.[8,9]

The carbon signal is complicated by the polypropylene substrate on which the cells lie, making the carbon signal a combination of cells plus substrate. The two carbon signals were naturally separated by the fitting since the spectral shape is characteristic of composition and polypropylene has an average composition almost exactly CH2. The polypropylene foil thickness is remarkably well determined in this analysis, with a measured (fitted) thickness non-uniformity of about 4.3% for all the measured samples, demonstrating that the fits are consistent between cells since this non-uniformity is characteristic of the foil itself.

Finally, since the irradiated area for each selected cell is precisely known, the areal density units can be expressed directly in units of mass. To interpret the EBS spectrum, the scattering cross-section functions for the various elements is needed. For Au the scattering is Rutherford, but for the others it is strongly non-Rutherford. Evaluated scattering cross-sections are available for the most important C, N, O and S:[10] measured cross-sections are used for Na[11] and P.[12]

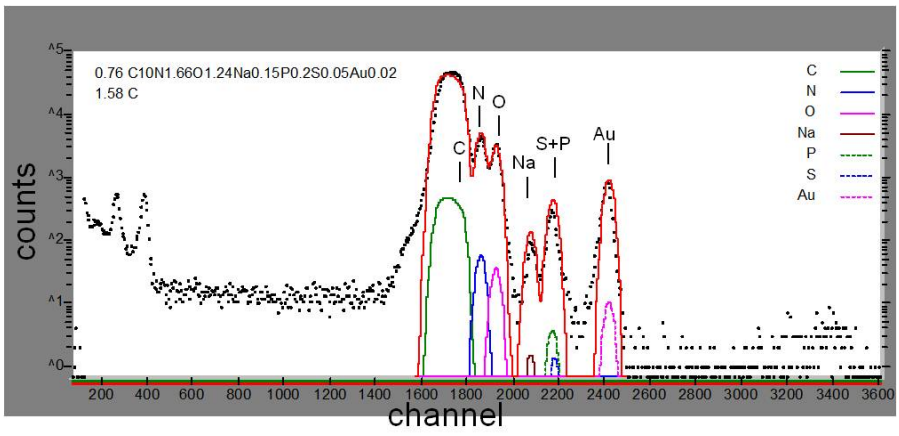

(a)

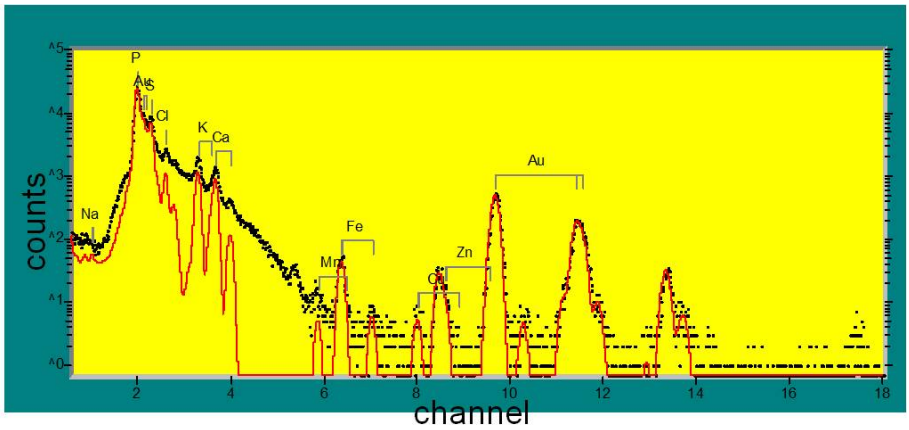

(b)

Figure S1: Typical IBA spectra from cells incubated with gold nanoparticles using OMDAQ software (a) Elastic backscattering spectrum (roughly fitted with OMDAQ) showing elements associated with living cells C, N, O, Na, S+P (there is no mass resolution to distinguish S & P). The Au is from the gold nanoparticles. (b) Proton-induced X-ray emission spectrum (fitted with GUPIX[1]) shows light elements (e.g. P, Ca, Cl) and trace elements (e.g Zn, Fe and Au from the GNPs). The signal from the sulphur K-line is not visible, being swamped by the gold M-line.

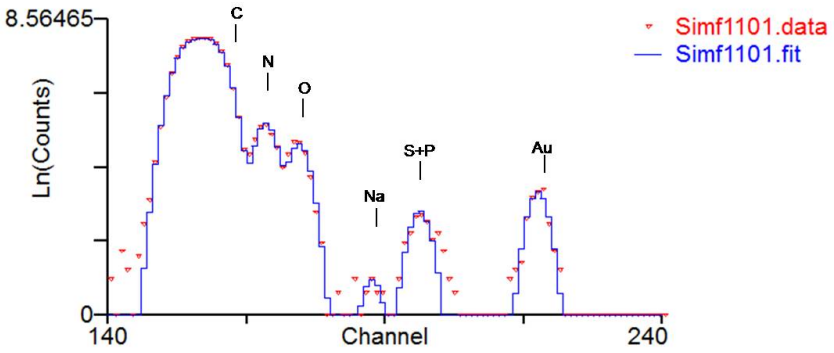

(a)

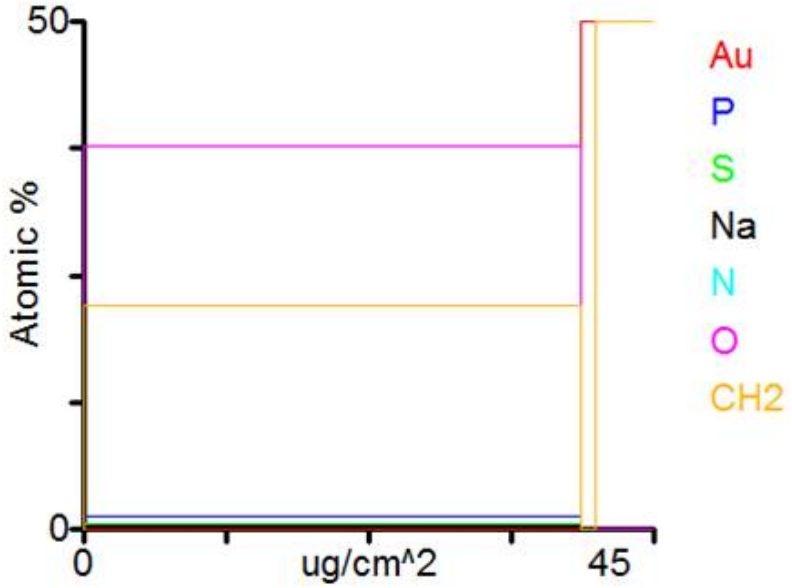

(b)

Figure S2: Analysis of individual cell spectrum with DataFurnace (a) Typical elastic backscattered spectrum of a cell fitted for C, N, O, Na, S+P and gold using a "layered" structure (b) The layered structure for fitting is shown giving % atomic percent of each element in μg /cm^2 for a single cell. To measure the gold content in pg in each cell, the data was normalised to the area of the cell.

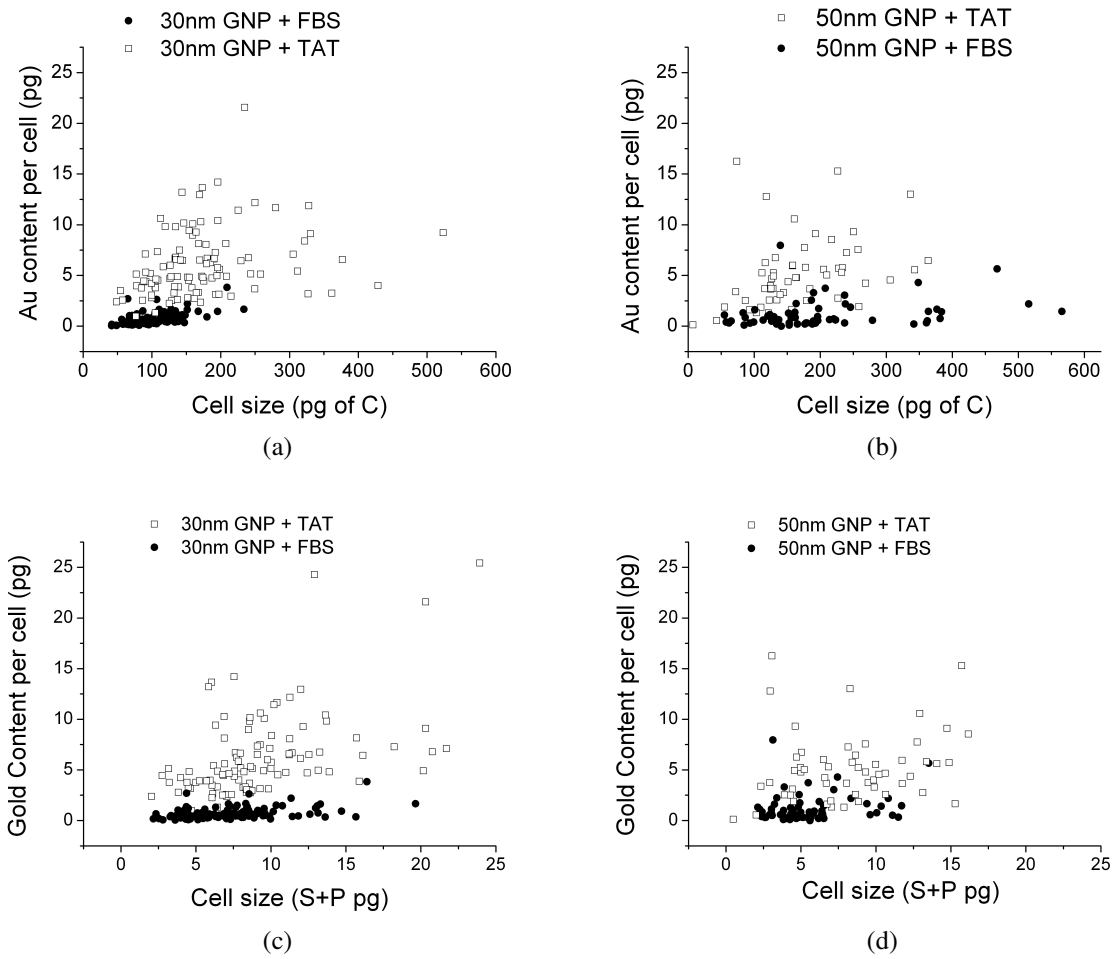

Figure S3: Scatter plot showing the mass of gold nanoparticles (pg of Au) with a FBS or TAT coating in individual cells with mass of each cell, either in pg of C (a & b) or pg of S+P (c & d). The data in 30nm + TAT was modelled which is shown in Figure 3 and the modelling section of the supplementary information.

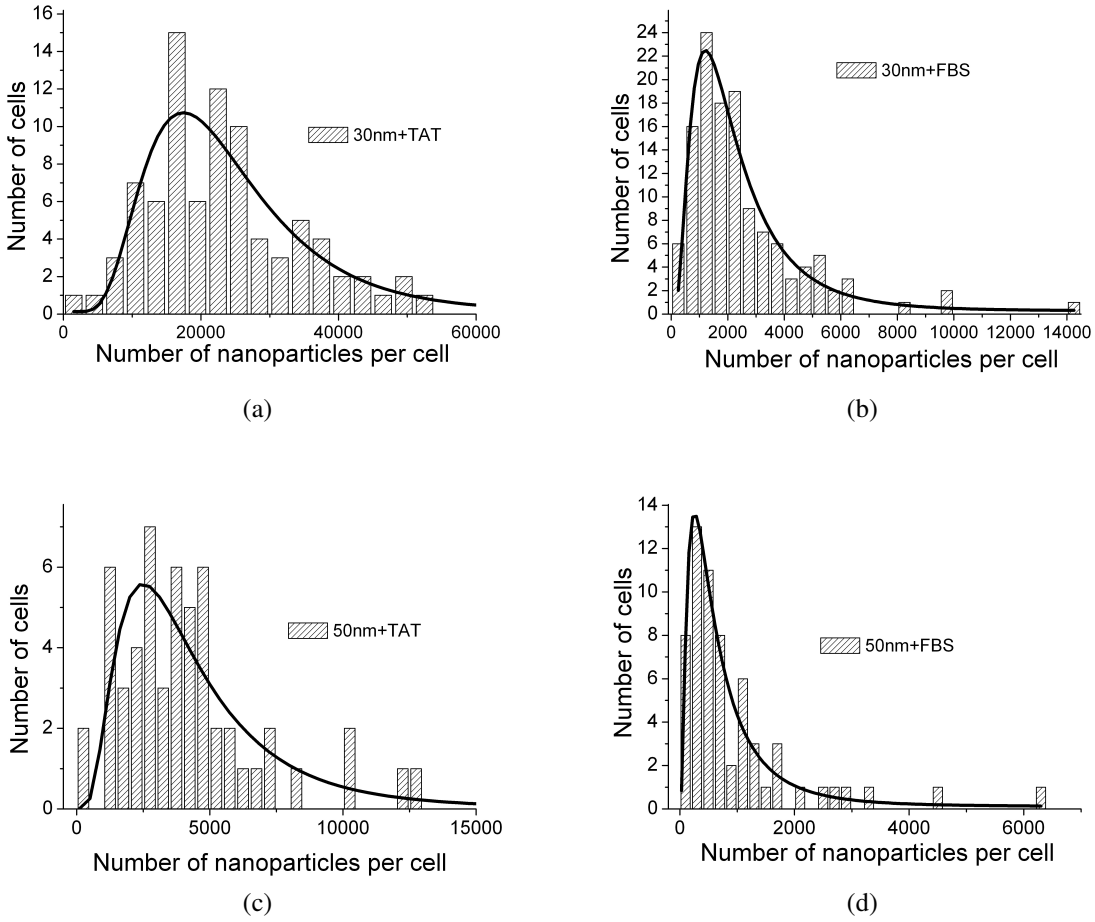

Figure S4: Histogram of the number of gold nanoparticles per cell incubated with (a) 30nm+TAT (b) 30nm+FBS (c) 50nm+TAT and (d) 50nm+FBS. The black lines shows the data fitted with a log-normal distribution (for log-normal fitting parameters see Table S2).

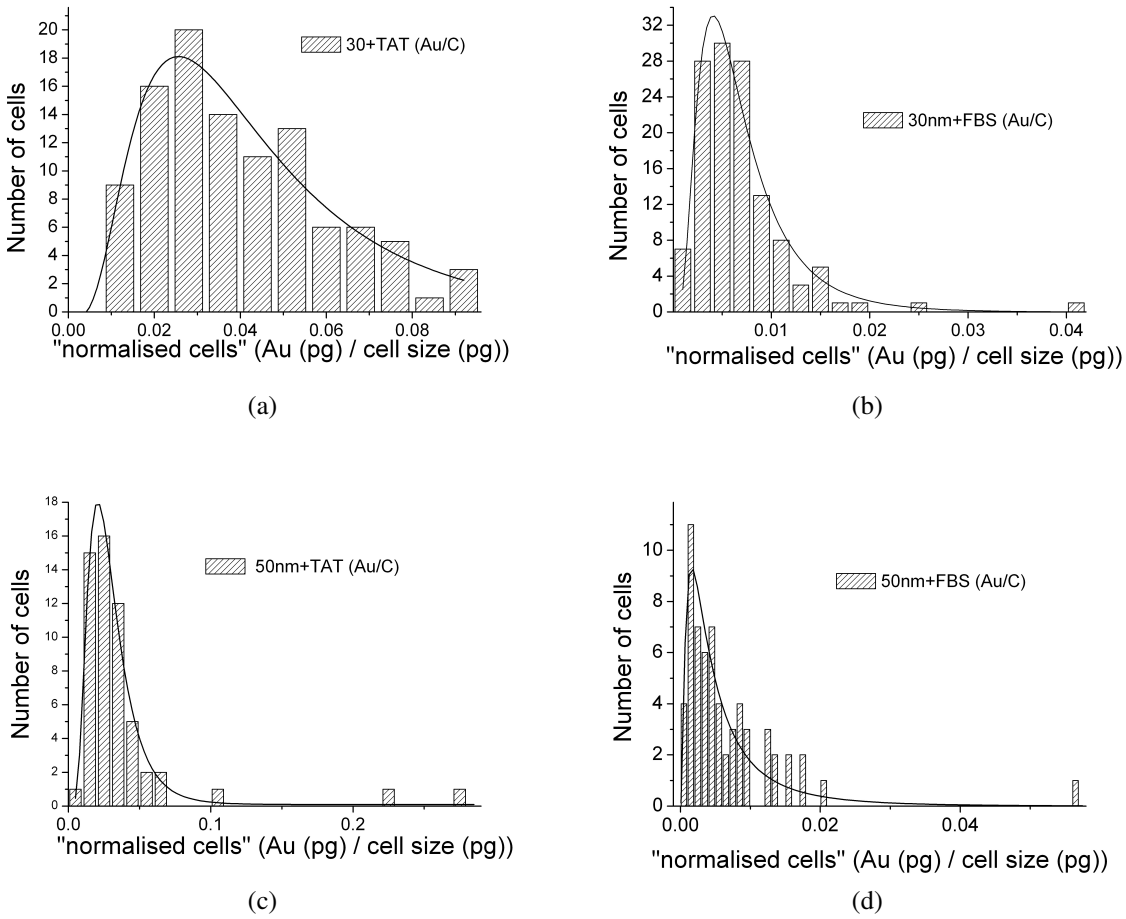

Figure S5: Histogram of the mass of gold in a "normalised cells", that is, the ratio of gold in a cell to its size (in terms of pg of carbon) (a) 30nm + TAT (b) 30nm + FBS (c) 50nm + TAT and (d) 50nm +FBS. The purpose of this is to determine whether cells of the same size can have a significantly different number of GNPs. The black lines are the data fitted with a log-normal distribution (for log-normal fitting parameters see Table S3).

Table S2: Log-normal fit parameters to the number of gold nanoparticles per cell, incubated with 30nm + FBS, 30nm+TAT, 50nm + FBS and 50nm+TAT GNPs (see Figure 4 and Table S3 for the histograms). xc is the centre of the peak, w equals 2 times the standard deviation normalised to the centre of the peak and A is the area under the curve.

50+TAT			
	Adj. R-Square	0.76	
		Value	Standard Error
	xc	3751	261
	w	0.64	0.059
	A	27296	2072
30+TAT			
	Adj. R-Square	0.80	
		Value	Standard Error
	xc	21829	1320
	w	0.47	0.058
	A	246051	23450
50nm + FBS			
	Adj. R-Square	0.92	
		Value	Standard Error
	xc	569	54
	w	0.89	0.06
	A	11559	727
30nm + FBS			
	Adj. R-Square	0.94	
		Value	Standard Error
	xc	1953	116
	w	0.69	0.05
	A	59451	3296

Table S3: Log-normal fit parameters to "normalised cells", incubated with 30nm + FBS, 30nm + TAT, 50nm + FBS and 50nm + TAT GNPs (see Figure 4 and Figure S4 for the histograms). This is the ratio of the mass of gold in a cell to its mass in carbon (Au (pg)/ C (pg)). The purpose of this is to determine whether cells of the same size can have a significantly different number of GNPs. xc is the centre of the peak, w equals 2 times the standard deviation normalised to the centre of the peak and A is the area under the curve.

30nm + FBS (Au/C)			
	Adj. R-Square	0.95	
		Value	Standard Error
	xc	0.006	2.89E-04
	w	0.62	0.049
	A	0.25	0.013
50nm + FBS (Au/C)			
	Adj. R-Square	0.88	
		Value	Standard Error
	xc	0.004	4.60E-04
	w	0.99	0.062
	A	0.062	0.003
30nm + TAT (Au/C)			
	Adj. R-Square	0.97	
		Value	Standard Error
	xc	0.038	0.004
	w	0.65	0.09
	A	0.01	0.001
50nm + TAT (Au/C)			
	Adj. R-Square	0.98	
		Value	Standard Error
	xc	0.03	5.00E-04
	w	0.5	0.02
	A	0.5	0.01
30nm + TAT (Au/C) Simulated data			
	Adj. R-Square	0.99	
		Value	Standard Error
	xc	0.036	0.004
	w	0.50	0.09
	A	0.01	0.001

Modeling and simulating GNP uptake in individual cells

A Monte Carlo simulation of uptake of gold nanoparticles was built using Python 2.7 (an open source programming language) to model the uptake of gold nanoparticles into individual cells over their life cycle. Important features of the simulation were; a log-normally distributed variation in the maximum velocity and Michaelis constant parameters of the Hill equation used to calculate the uptake rate of gold nanoparticles and a log-normal distribution of cell size. The Hill equation was chosen to describe uptake rate, after finding that it fitted Chithrani *et al.*'s[13] data excellently. This fit is shown in Figure S6, the parameter are shown in Table S4, and the equation is shown in equation 1. The Hill model is appropriate in terms of biological relevance, as it can describe the kinetics of receptor-to-ligand bindings. This is relevant to GNP uptake as it is known that GNPs bind to receptors on the cell surface, before being invaginated into the cell and stored in lysosomes. We acknowledge that the Hill model is a simplistic analytical approach to modelling GNP uptake, and that more advanced numerical models exist.[14] Because of the complexity of the receptor mediated endocytosis for intracellular NP uptake shown in studies (e.g.[15]), there is not yet sufficient understanding of the parameters of such numerical models. Many simplifications are necessary; consequently the simple analytical Hill model is an good "first iteration" model to describe the GNP uptake process. In addition, it works well.

$$y = V_{max} + (V_{min} - V_{max})\frac{x^h}{k^h + x^h} \tag{1}$$

As the sampling of our data was taken at 48 hours, we had to take into account cell division into our model. We simulated cells dividing their mass and GNP content between daughter cells using binomial statistics to share GNP content on division[16] after 20 hours and repopulating their GNP content from this point. As can be seen in the fits in Figure S6a, the cells repopulate their GNP content after about 10 hours before the rate of uptake reaches a plateau. Cells do not have an ever increasing "plateau" region of GNPs content on division, but instead reach a maximum steady

state. In terms of the mechanics of the model this is a necessity. We can explain it by assuming that as the newly divided cell grows, it rapidly makes new unsaturated endocytosis receptors which can import GNPs from the media. As the cell ages, the rate of creation of these new receptors slows (possibly because the cell grows less quickly) and so a plateau region is reached. The cell then divides and the process begins again. In this way, we modelled the rate of uptake for our data by fitting the mode number of GNPs we measured at 48 hours. This can be seen in Figure S6b.

Table S4: The Hill fitting parameters to Chithrani *et al* and the data in this paper. For the Chithrani *et al* data, the adjusted R-squared values indicating "goodness of fit" are all >0.98. The scaling factor refers to log-normal distribution of uptake rate to relate the Michaelis parameter (k) and maximum velocity (V) parameter of the Hill equation proportionally. The dimensionless h refers to the Hill constant, Vmin and Vmax refer to the reaction velocity of the uptake rate.

	Chithrani et al			Jeynes et al			
nm	**50**	**74**	**14**	**30 + FBS**	**50 + FBS**	**30 + TAT**	**50 + TAT**
Vmax (GNP/hour)	1867.30	935.84	1302.63	599.78	174.74	6703.83	1151.96
Vmin (GNP/hour)	-775.98	-388.75	-541.11	-249.25	-72.62	-2785.86	-478.71
k (GNP)	4722.39	2364.06	3290.61	1516.84	441.93	16953.95	2913.29
h	2.99	2.99	2.99	2.99	2.99	2.99	2.99
Scaling factor	1.00	0.50	0.70	0.32	0.09	3.59	0.62

Next, we simulated the scatter of the data seen when cell mass is plotted against cell GNP content (see Figure S3). We simulated cells which had a log-normally distributed mass and a log-normally distributed rate of 30nm+TAT GNP uptake, "growing" them at 6 minute time intervals over 48 hours. The resultant scatter plot at 48 hours can be seen in Figure 3.

This material is available free of charge via the Internet at `http://pubs.acs.org/`.

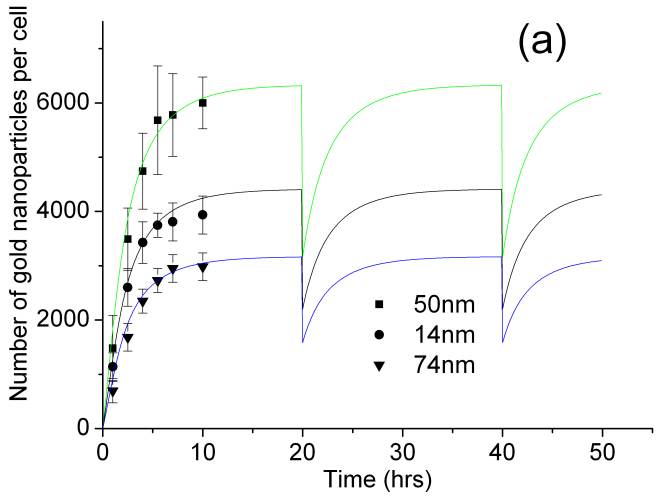

(a)

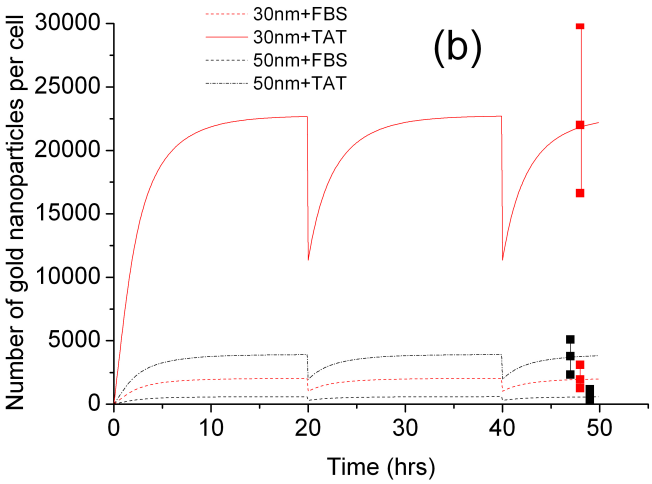

(b)

Figure S6: (a) Data from Chithrani *et al.* was fitted using a Hill equation. Each of the three nanoparticle sizes have the same Hill constant parameter, which describes the binding affinity of the nanoparticles to the receptors. The Hill fit is shown by the lines while the parameters of the Hill fit are shown in Table S4. In the model the cells divide at 20 hours.(b) The data for our paper was taken at 48 hours (in the graph the data positions are slightly shifted for clarity). Here the Hill equation is used to fit the mode number of GNPs in each of the samples. The square data points joined by a vertical line represent the mode and 25% and 75% percentiles. The cells reach a "plateau" according to the data which fits well with the Hill equation. Our model predicts that this "plateau" is a maximum in terms of how many GNP a cell can contain, no matter how many times a cell divides. We can explain it by assuming that as the newly divided cell grows, it rapidly makes new unsaturated endocytosis receptors which can import GNPs from the media, giving an initial rapid uptake of GNPs. As the cell ages, the rate of creation of these new receptors slows (possibly because the cell grows less quickly) and so a plateau region is reached. The cell then divides and the process begins again.

References

(1) Campbell, J. L.; Boyd, N. I.; Grassi, N.; Bonnick, P.; Maxwell, J. A. *Nucl. Instrum. Methods B* **2010**, *268*, 3356–3363.

(2) Jeynes, C.; Bailey, M. J.; Bright, N. J.; Christopher, M. E.; Grime, G. W.; Jones, B. N.; Palitsin, V. V.; Webb, R. P. *Nucl. Instrum. Methods B* **2012**, *271*, 107–118.

(3) Garman, E. F.; Grime, G. W. *Prog. Biophys. Mol. Biol.* **2005**, *89*, 173–205.

(4) Grime, G. *Nucl. Instr. Methods B* **1996**, *109-110*, 170–174.

(5) Barradas, N. P.; Jeynes, C. *Nucl. Instrum. Methods B* **2008**, *266*, Inter Univ Accelerator Ctr; Inst Phys.

(6) N.P., B. *J. Phys. D: Appl. Phys.* **2001**, *34*, 2109–16.

(7) Bragg, W. H.; Kleeman, R. *Philos. Mag.* **1905**, *10*, 318.

(8) Ziegler, J. F.; Ziegler, M. D.; Biersack, J. P. *Nucl. Instrum. Methods B* **2010**, *268*, 1818–1823.

(9) `www.SRIM.org`.

(10) Gurbich, A. F. *Nucl. Instrum. Methods B* **2010**, *268*, 1703–1710.

(11) Vanhoy, J.; Bilpuch, E.; Westerfeldt, C.; Mitchell, G. *Phys. Rev. C* **1987**, *36*, 920–932.

(12) Fang, D.; Bilpuch, E.; Westerfeldt, C.; Mitchell, G. *Phys. Rev. C* **1988**, *37*, 28–40.

(13) Chithrani, B. D.; Ghazani, A. A.; Chan, W. C. W. *Nano Lett.* **2006**, *6*, 662–668.

(14) Dobay, M. P. D.; Alberola, A. P.; Mendoza, E. R.; Raedler, J. O. *J. Nano. Res.* **2012**, *14*.

(15) Rudolf, N.; Ohlsson-Wilhelm, B.; Leary, J.; Rowley, P. *Cytometry* **1985**, *6*, 151–158.

(16) Summers, H. D.; Rees, P.; Holton, M.; Brown, M. R.; Chappell, S. C.; Smith, P. J.; Errington, R. J. *Nature Nano.* **2011**, *6*, 170–174.